Journal of Luminescence 251 (2022) 119214

Contents lists available at ScienceDirect

Journal of Luminescence

journal homepage: www.elsevier.com/locate/jlumin

Full Length Article

Probing carrier concentration of doped GaN single crystals from LO phonon-plasmon coupled modes

Linxuan Li, Siqi Zhu, Lu Cheng, Hongsheng Qi, Yu Fan, Wei Zheng *

State Key Laboratory of Optoelectronic Materials and Technologies, School of Materials, Sun Yat-sen University, Guangzhou, 510275, China

ARTICLE INFO

Keywords:
Carrier concentration
LOPC mode
GaN
Raman spectra
Infrared reflectance spectra

ABSTRACT

Raman and infrared reflectance spectroscopy were used to study GaN single crystals with different doping types and carrier concentrations. In different samples, the characteristic spectra related to LO phonon-plasmon coupled (LOPC) mode are observed as changing regularly with carrier concentration. Furthermore, to obtain the carrier concentration and mobility of GaN crystals, Raman and infrared reflectance spectra with LOPC modes were fitted. The carrier concentration obtained agrees well with that obtained from the Hall measurement, which confirms that these non-contact and non-destructive spectroscopy methods with high spatial resolution are reliable to probe the carrier concentration of doped GaN single crystals.

1. Introduction

As a third-generation semiconductor, gallium nitride (GaN) has received extensive attention in recent years. Compared with traditional semiconductor silicon, GaN owns the characteristics of a larger bandgap (3.39 eV), higher critical breakdown electric field (2.5 MV·cm^{-1}), and greater electron saturation drift velocity (2.5 × 10^{7} cm·s^{-1}) [1,2], which endows it with unique advantages in ultraviolet optoelectronics [3–6] and high-power [7,8] and radio-frequency [9] electronics applications.

To design an electronic device with required performance, carrier concentration and mobility should be precisely measured. In the polar semiconductor GaN, when longitudinal optical (LO) phonons and plasmons have the same electric field direction and similar frequencies, an obvious coupling effect will occur to form a LO phonon-plasmon coupled (LOPC) mode, which can be observed in infrared reflectance or Raman spectra [10]. When carrier concentration increases, both peak position and linewidth of LOPC mode in spectra will change simultaneously, which can assist in extracting carrier concentration and mobility [11–15]. Compared with the widely-used Hall measurement, these spectroscopy methods own the advantages of being non-contact and damage-free since the ohmic electrodes are unnecessary. Therefore, for the measurement of the electronic parameters of GaN single crystals, spectroscopy methods are expected to be more applicable than electrical methods [10,16].

There have been some researches using Raman spectroscopy to characterize the electrical properties of GaN, but most studied samples are thin films [1,17–19] or have a narrow carrier concentration range or single doping type (Si-doped mainly) [18,20–22]. Raman spectroscopy characterization of electrical properties of bulk GaN crystals with a wide carrier concentration range and diverse doping types is still worthy of research. In addition, studies that apply infrared reflectance spectroscopy to characterize the carrier concentration and mobility of GaN are rarely conducted [10,19], which also proves the necessity of further study.

In this article, both Raman and infrared reflectance spectra are applied to measure bulk GaN single crystals with different doping types (Fe-, Si-, Ge-doped and undoped) and carrier concentrations (10^{16}-10^{18} cm^{-3}). In the analysis of Raman spectra, the dependence of LOPC mode frequency on carrier concentration is established according to the dielectric function, which can effectively predict the behavior of LOPC modes in different carrier concentration samples. Furthermore, the lineshape of LOPC^{+} mode is fitted through a Raman intensity relationship, based on which we get the mobility and carrier concentration. The electrical properties are also extracted from the infrared reflectance spectra through the relationship between reflectivity and dielectric function. Comparing the results obtained from Raman and infrared reflectance spectra with those from the Hall measurement, it is found that the carrier concentrations achieved from these three ways agree well while the mobility does not. The possible reasons for the mobility discrepancy are discussed.

Abbreviations: LOPC, LO phonon-plasmon coupled.

* Corresponding author.
E-mail address: zhengw37@mail.sysu.edu.cn (W. Zheng).

https://doi.org/10.1016/j.jlumin.2022.119214
Received 10 June 2022; Received in revised form 30 July 2022; Accepted 10 August 2022
Available online 14 August 2022

2. Materials and methods

Four bulk GaN single crystals were grown by hydride vapor phase epitaxy (HVPE) method with the same size of 10 × 10 × 0.35 mm^3 and different doping types (Fe-, Si-, Ge-doped and undoped), all of which were from Suzhou Nanowin Science Technology Co., Ltd. These samples grew along the *c*-axis with (0001) plane and were epitaxially polished to achieve optical quality. Carrier concentration and mobility of these four samples were measured by the Hall measurement at room temperature (Table 1). It is noted that valid data of GaN: Fe sample cannot be obtained due to its low carrier concentration (n~10^{16} cm^{-3}).

Raman spectra were measured through a Renishaw spectrometer (InVia Reflex) with a resolution of 1.5 cm^{-1}, during which an Ar-ion laser at 488 nm was used for excitation. The laser was incident perpendicularly on the (0001) plane of the crystals with the backscattering geometric configuration. Infrared reflectance spectra were obtained via a Fourier transform infrared spectrometer (Shimadzu IRAffinity-1S). This measurement was performed on the (0001) plane of the crystals at 10° incidence. A gold mirror was applied for background scanning. Both the Raman and infrared measurements were performed at room temperature.

3. Results and discussion

3.1. Analysis of Raman spectra

Fig. 1(a) shows Raman spectra of the four bulk GaN crystals with different doping concentrations, where both A_1(LO) and E_2(high) modes can be observed [23]. Since GaN: Fe sample has a relatively low carrier concentration (n~1 × 10^{16} cm^{-3}), A_1(LO) mode will not couple with plasmon or shift to high frequency [24]. Therefore, the frequency of A_1(LO) Raman peak (731 cm^{-1}) obtained by Lorentz fitting of GaN: Fe can be taken as that of uncoupled A_1(LO) mode, whose value corresponds with that of the reported research [24]. In addition, the A_1(LO) mode coupled with plasmon forming $LOPC^+$ mode exhibits blueshift and broadening with increasing concentration in undoped, Ge-doped, and Si-doped GaN, as shown in the inset of Fig. 1(a). To study the lineshape of this coupled mode, we started from the dielectric function as follows [25]:

$$\varepsilon_r(\omega) = \varepsilon_\infty + \varepsilon_\infty \frac{\omega_{LO}^2 - \omega_{TO}^2}{\omega_{TO}^2 - \omega^2 - i\omega\Gamma} - \varepsilon_\infty \frac{\omega_P^2}{\omega(\omega + i\gamma)} \quad (1)$$

where ε_∞ is the high-frequency dielectric constant. γ and Γ are the plasmon and phonon damping constants, respectively. ω_{TO} (533 cm^{-1}) and ω_{LO} (731 cm^{-1}) are transverse optical (TO) and LO phonon frequencies [26]. ω_P is the plasmon frequency. The second term in Eq. (1) comes from lattice vibration and the third term is from plasmon. ω_P is related to the free carrier concentration *n*, which can be expressed as:

$$\omega_P = \left(\frac{4\pi n e^2}{\varepsilon_\infty m^*}\right)^{1/2} \quad (2)$$

where m^* is the effective mass, and $m^* = 0.19\ m_0$ for GaN [27]. If only consider the excitations near the Brillouin zone center ($q \cong 0$) and neglected damping terms γ and Γ, Eq. (1) can be simplified and written

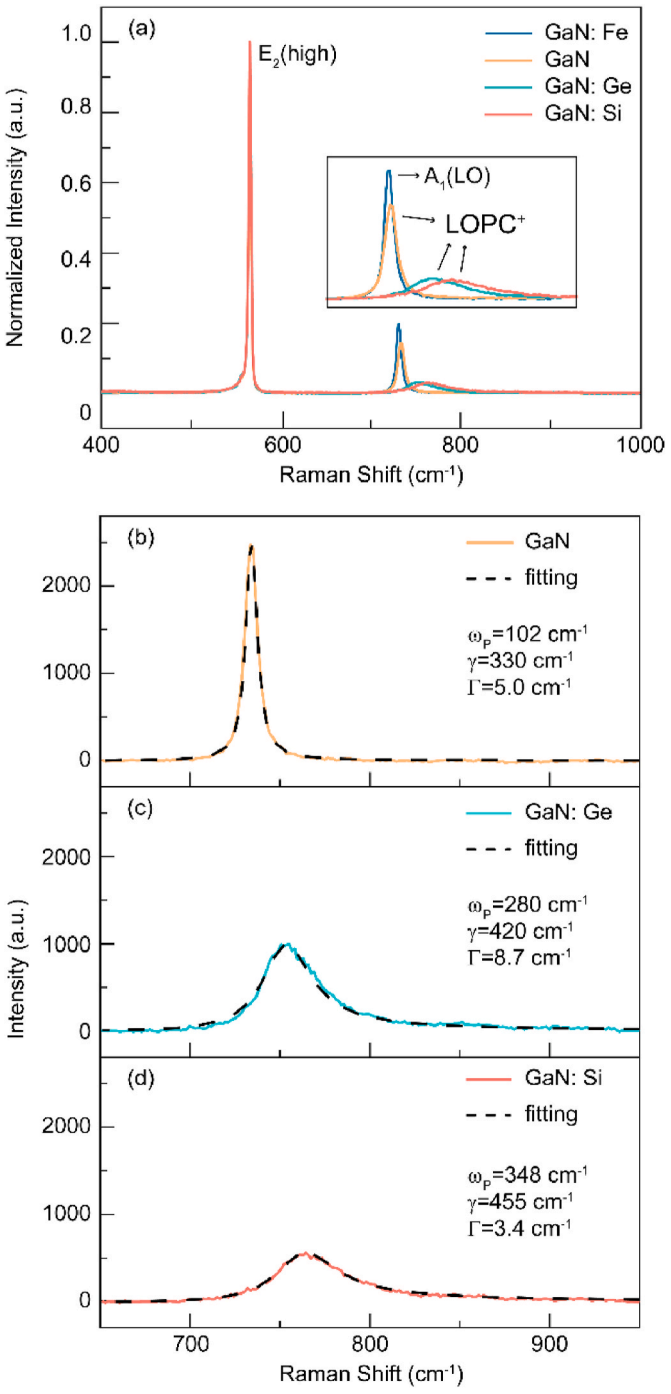

Fig. 1. Analysis of Raman spectra of GaN single crystals with different carrier concentrations. (a) The experimental Raman spectra of samples; The experimental (solid line) and fitting (dash line) curves of (b) undoped GaN, (c) GaN: Ge, and (d) GaN: Si.

Table 1
Carrier concentrations and mobility of the four bulk GaN single crystals obtained from the Hall, Raman, and infrared reflectance measurements.

Sample	Hall		Raman (A_1 mode)		Infrared reflectance (E_1 mode)	
	Carrier concentration (cm^{-3})	Mobility ($cm^2 \cdot V^{-1} \cdot s^{-1}$)	Carrier concentration (cm^{-3})	Mobility ($cm^2 \cdot V^{-1} \cdot s^{-1}$)	Carrier concentration (cm^{-3})	Mobility ($cm^2 \cdot V^{-1} \cdot s^{-1}$)
GaN: Si	1.36 × 10^{18}	355	1.37 × 10^{18}	108	1.72 × 10^{18}	98
GaN: Ge	7.01 × 10^{17}	407	8.89 × 10^{17}	117	9.53 × 10^{17}	123
GaN	1.18 × 10^{17}	777	1.18 × 10^{17}	149	1.37 × 10^{17}	175
GaN: Fe	–	–	–	–	–	–

as $\varepsilon(\omega) = 0$ [2]. The frequency of LOPC mode ω_{LOPC} is the root of this equation. Solving this equation, we can get the relationship between ω_{LOPC} and ω_P [15]:

$$\omega_{LOPC}^2 = \frac{1}{2}\left\{\omega_P^2 + \omega_{LO}^2 \pm \left[\left(\omega_P^2 + \omega_{LO}^2\right)^2 - 4\omega_P^2\omega_{TO}^2\right]^{\frac{1}{2}}\right\} \quad (3)$$

Eq. (3) indicates that the LOPC mode in GaN can split into two modes, that are, LOPC$^+$ and LOPC$^-$. Fig. 2 shows the relationship between LOPC mode frequency ω_{LOPC} and carrier concentration n. From the red solid lines calculated by Eq. (3), as carrier concentration increases, for LOPC$^+$ mode, it moves to the high frequency and gets away from ω_{LO}; for LOPC$^-$ mode, it also moves to high frequency but approaches ω_{TO}. In this work, aside from the LOPC$^+$ mode, the weak LOPC$^-$ mode is observed in the spectra with logarithmic coordinates in GaN: Si and GaN: Ge samples. Both LOPC$^+$ and LOPC$^-$ mode frequencies shown in Fig. 2 are in line with the theoretical equation when $n < 10^{18}$ cm^{-3}; however, when $n > 10^{18}$ cm^{-3}, a slight discrepancy is observed.

The above results verify that the correlation between LOPC Raman shift and carrier concentration shown in Eq. (3) can be used to estimate samples' carrier concentration, especially for those with a low carrier concentration, of which the plasmon damping is low enough to be ignored. For samples with a high carrier concentration, since LOPC mode in Raman spectra (Fig. 1(a)) is greatly affected by plasmon damping, merely using ω_{LOPC} as the input parameter is not sufficient to obtain a reliable estimate of carrier concentration, and lineshape fitting taking account of plasmon damping must be applied instead.

An intensity equation is constructed to extract the carrier concentration of GaN by fitting the LOPC Raman peak, which can also obtain carrier mobility μ. In the Raman scattering of polar semiconductors, there are three mechanisms for LOPC mode to interact with incident light: deformation-potential + electro-optic (DP + EO) mechanism, charge density fluctuation (CDF) mechanism, and impurity induction (IIF) mechanism [14]. The DP + EO mechanism describes how atomic displacements and macroscopic longitudinal field modulate the polarizability; the CDF mechanism describes the scattering caused by the fluctuation of charge density; the IIF mechanism describes how the effect between electrons and phonons caused by impurities affects scattering process. Among these three mechanisms, the contribution of DP + EO mechanism is predominant in GaN, according to the relevant research [1]. Considering this mechanism only, the intensity of LOPC peak can be expressed as [28,29]:

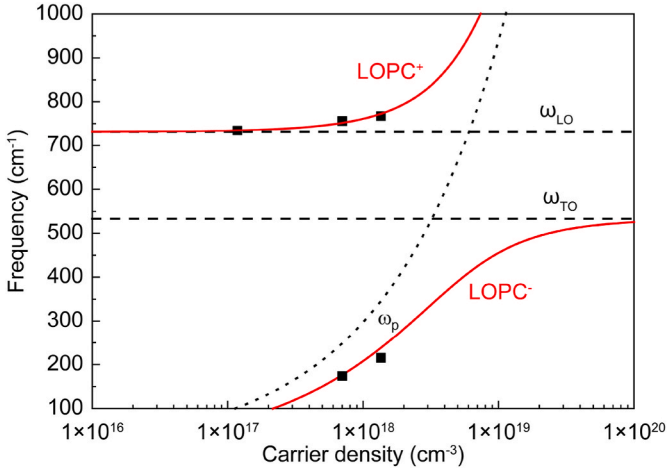

Fig. 2. The LO phonon-plasmon coupled interaction in GaN. The red solid lines indicate that the LOPC mode depends on carrier concentration, which are calculated by Eq. (3). The dotted line shows the plasmon frequency ω_P, which is calculated from Eq. (2). The black solid dots come from the Hall and Raman measurements.

$$I(\omega) = const \cdot A(\omega) \cdot \mathrm{Im}\left[-\varepsilon_r(\omega)^{-1}\right] \quad (4)$$

where ω is the Raman shift, and $A(\omega)$ is given by:

$$\begin{aligned} A(\omega) &= 1 + 2C\frac{\omega_{TO}^2}{\delta}\left[\omega_P^2\gamma\left(\omega_{TO}^2 - \omega^2\right)\right. \\ &-\omega^2\Gamma\left(\omega^2 + \gamma^2 - \omega_P^2\right) \\ &+C^2\left\{\omega_P^2\left[\gamma\left(\omega_{LO}^2 - \omega_{TO}^2\right) + \Gamma\left(\omega_P^2 - 2\omega^2\right)\right]\right. \\ &+\omega^2\Gamma\left(\omega^2 + \gamma^2\right)\left[\frac{\omega_{TO}^4}{\delta\left(\omega_{LO}^2 - \omega_{TO}^2\right)}\right] \\ \delta &= \omega_P^2\gamma\left[(\omega\Gamma)^2 + \left(\omega_{TO}^2 - \omega^2\right)^2\right] \\ &+\omega^2\Gamma\left(\omega^2 + \gamma^2\right)\left(\omega_{LO}^2 - \omega_{TO}^2\right) \end{aligned} \quad (5)$$

where C is the Faust-Henry coefficient. The electron mobility μ can be obtained from plasmon damping constant γ by the following equation:

$$\gamma = \frac{e}{m^*\mu} \quad (6)$$

It should be noted that the mobility is anisotropic since GaN is a uniaxial crystal. The mobility obtained through Hall measurement was in-plane. As for the spectroscopy methods, the direction of the fitting mobility depends on the phonon vibration direction, as the measured phonon is coupled with plasmon. In the Raman measurement, the A_1(LO) mode vibrates along the c-axis, so we got the out-of-plane mobility. In the infrared measurement, the E_1(LO) mode coupled with the plasmon vibrates perpendicular to the c-axis, so the obtained mobility is the in-plane one (see details in section 3.2). For GaN, its effective mass can be written as $m^* = [(1/3)(1/m_{\parallel}) + (2/3)(1/m_{\perp})]^{-1}$ ($m_{\parallel}$ and $m_{\perp}$ are the parallel and perpendicular effective mass, respectively). However, since there is little difference between the perpendicular $m_{\perp}$ and parallel effective mass $m_{\parallel}$ of GaN [30,31], we considered the mobility of GaN as isotropic and simplified the mobility calculation in Raman and infrared spectra by using the same effective mass, that is $m^* = 0.19\ m_0$ [27]. $C = 0.48$, $\varepsilon_\infty = 5.35$ are taken for the Raman fitting [18,24,27]. Based on Eqs. (1), (2), (4)-(6) and choosing γ, Γ, and ω_P as fitting parameters, the free carrier concentration and mobility can be obtained.

In this research, we focus on LOPC$^+$ branch. Since the carrier concentration of sample GaN: Fe is too low that the A_1(LO) mode is uncoupled, it cannot be fitted by this way. The LOPC$^+$ peaks and fitting curves of undoped GaN, GaN: Ge, and GaN: Si samples are shown in Fig. 1(b)–(d). As carrier concentration increases, the LOPC$^+$ mode shows blueshift and broadening, which means LOPC effect is strengthened. The fitting curves well correspond to the experimental results. The carrier concentrations and mobility gotten from Raman spectra are shown in Table 1.

3.2. Analysis of infrared reflectance spectra

Fig. 3(a) shows the infrared reflectance spectra of the four bulk GaN crystals. Since the light is incident from the (0001) plane, the observed phonons in infrared reflectance spectra are E_1 modes [10]. Phonon polaritons formed by coupling the E_1(TO) phonons and the photons result in a reststrahlen band with strong reflection, whose frequency is between ω_{TO} and ω_{LO} [32]. The high-frequency edge of reststrahlen band becomes smooth as the carrier concentration increases, for LOPC mode formed by the coupling of E_1(LO) and plasmon will affect the behavior of phonon polaritons. Thus, we can get the carrier concentrations of GaN by fitting the infrared spectra.

At the junction between vacuum or air and solid surfaces, vertical and parallel reflectivity are considered respectively as follows [33,34]:

This equation is same with the following one, please delete this repeated equation.

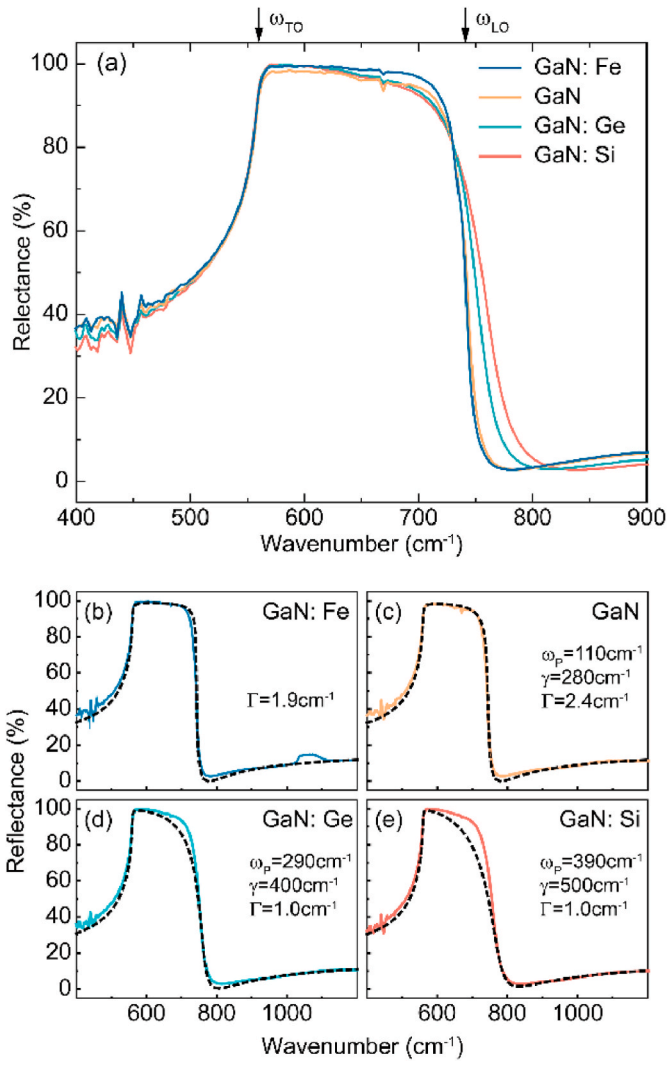

Fig. 3. Analysis of infrared reflectance spectra of GaN single crystals with different carrier concentration. (a) The experimental infrared reflectance spectra of samples; The experimental (solid line) and fitting (dash line) curves of (b) GaN: Fe, (c) undoped GaN, (d) GaN: Ge, and (e) GaN: Si.

$$R_s = \left|\frac{cos\theta_i - \sqrt{\varepsilon - sin^2\theta_i}}{cos\theta_i + \sqrt{\varepsilon - sin^2\theta_i}}\right|^2$$
$$R_p = \left|\frac{\varepsilon cos\theta_i - \sqrt{\varepsilon - sin^2\theta_i}}{\varepsilon cos\theta_i + \sqrt{\varepsilon - sin^2\theta_i}}\right|^2 \quad (7)$$

where θ_i is the incident angle, which is 10° in the infrared measurement. Here, it can be approximated to normal incidence ($\theta_i = 0°$) within allowable error range. The reflectivity of light at normal incidence is:

$$R(\omega) = R_s = R_p = \frac{[\eta(\omega) - 1]^2 + \kappa(\omega)^2}{[\eta(\omega) + 1]^2 + \kappa(\omega)^2} \quad (8)$$

where $\kappa(\omega)$ and $\eta(\omega)$ refer to extinction coefficient and refractive index, respectively, which are related to the dielectric function as:

$$\varepsilon_r(\omega) = [\eta(\omega) + i\kappa(\omega)]^2 \quad (9)$$

The infrared reflectance spectra of GaN, GaN: Ge, and GaN: Si can be fitted using Eqs. (1), (8) and (9) as fitting functions with ω_P, Γ, and γ as fitting parameters. However, it should be noted that this method cannot obtain a valid carrier concentration for GaN: Fe with a low carrier concentration (n~10^{16} cm^{-3}) since E_1(LO) and plasmon are weak coupling. The dielectric function of GaN: Fe should omit the carrier term, yielding the equation [35]:

$$\varepsilon_r(\omega) = \varepsilon_\infty + \varepsilon_\infty \frac{\omega_{LO}^2 - \omega_{TO}^2}{\omega_{TO}^2 - \omega^2 - i\omega\Gamma} \quad (10)$$

The infrared reflectance spectra of samples with low carrier concentration can be fitted by using Eqs. (8)–(10) with Γ as the only fitting parameter. The frequencies of E_1(TO) and E_1(LO) are taken as 560 cm^{-1} and 741 cm^{-1} in the fitting of four samples [36–38]. The fitting curves are shown in Fig. 3(b)–(e) by dashed lines, and the obtained results are summarized in Table 1. The fitting curves are consistent with the experimental curves in the range of $\omega > 750$ cm^{-1}. It is worth noting that as carrier concentration increases, the fitting curve shows a certain deviation from the experimental curve around 700 cm^{-1}. The main reason is that the dielectric function in Eq. (1) is simplified by assuming TO-phonon damping equals LO-phonon damping [39]. In fact, for doped semiconductors, LO-phonon damping will increase with impurity concentration while TO-phonon damping is almost independent of that [16, 40].

3.3. Comparison

Table 1 summarizes the carrier concentrations and mobility tested by Hall, Raman, and infrared reflectance measurements. For the range of $n > 10^{17}$ cm^{-3}, a good consistency is shown among the carrier concentrations obtained from these three methods. However, the mobility obtained by spectroscopy methods is lower than that obtained by the electrical method, which the following reasons may cause. One reason may be that the assumption that TO-phonon damping is equal to LO-phonon damping in the dielectric function model does not reflect the actual situation well. Especially when the doping concentration increases, LO-phonon damping increases significantly while TO-phonon damping does not [40]. Also, when considering the distribution of carrier velocities, Hall mobility is no longer equal to drift mobility obtained from Raman and infrared measurements, and the ratio of Hall mobility and drift mobility depends on the scattering mechanism [41]. Another possible reason is that the carriers are in an equilibrium state in the Hall measurement, while in Raman or infrared reflectance measurement, they are in a non-equilibrium state due to light excitation [19]. This may cause a difference in the predominant carrier scattering mechanism among different methods, resulting in higher plasmon damping constants of Raman and infrared reflectance measurements than that of Hall measurement. Thus, the optical mobility will be lower.

4. Conclusions

In conclusion, Raman and infrared reflectance spectroscopy are used to study GaN single crystals with different doping types (Fe, Ge, Si-doped, and undoped) and carrier concentrations. The relationship between Raman shift of LOPC mode and carrier concentration is studied, which is suitable for preliminarily estimating the carrier concentration of low carrier concentration samples. For the samples with a carrier concentration greater than 10^{17} cm^{-3}, the Raman and infrared reflectance spectra with LOPC mode of GaN crystals are fitted to obtain their carrier concentrations and mobility. Comparing the Hall, Raman, and infrared results, it is found that the carrier concentrations extracted from these three ways show a good consistency while the mobility does not. The low mobility in spectroscopy methods may come from the carrier scattering mechanisms and the adopted simplification made in the dielectric function. These results show that Raman and infrared reflectance spectroscopy can be confirmed as reliable methods for measuring the carrier concentration of GaN single crystals.

Author Contributions

Linxuan Li: Investigation, Formal analysis, Methodology, Writing – original draft; **Siqi Zhu:** Writing – review & editing,; **Lu Cheng:** Data curation, Methodology. **Hongsheng Qi:** Methodology, **Yu Fan:** Methodology, **Wei Zheng:** Conceptualization, Funding acquisition, Supervision.

Declaration of competing interest

The authors declare that they have no known competing financial interests or personal relationships that could have appeared to influence the work reported in this paper.

Data availability

Data will be made available on request.

Acknowledgments

This work was financially supported by the Guangdong Natural Science Funds for Distinguished Young Scholars (No. 2021B1515020105).

References

[1] T. Kozawa, T. Kachi, H. Kano, Y. Taga, M. Hashimoto, N. Koide, K. Manabe, Raman scattering from LO phonon-plasmon coupled modes in gallium nitride, J. Appl. Phys. 75 (1994) 1098–1101, https://doi.org/10.1063/1.356492.
[2] P. Perlin, J. Camassel, W. Knap, T. Taliercio, J.C. Chervin, T. Suski, I. Grzegory, S. Porowski, Investigation of longitudinal-optical phonon-plasmon coupled modes in highly conducting bulk GaN, Appl. Phys. Lett. 67 (1995) 2524–2526, https://doi.org/10.1063/1.114446.
[3] W. Song, J. Chen, Z. Li, X. Fang, Self-powered MXene/GaN van der Waals heterojunction ultraviolet photodiodes with superhigh efficiency and stable current outputs, Adv. Mater. 33 (2021) 2101059, https://doi.org/10.1002/adma.202101059.
[4] L. Jia, W. Zheng, F. Huang, Vacuum-ultraviolet photodetectors, PhotoniX 1 (2020), https://doi.org/10.1186/s43074-020-00022-w.
[5] W. Zheng, L. Jia, F. Huang, Vacuum-Ultraviolet Photon Detections, iScience 23 (2020), 101145, https://doi.org/10.1016/j.isci.2020.101145.
[6] W. Zheng, R. Lin, J. Ran, Z. Zhang, X. Ji, F. Huang, Vacuum-ultraviolet photovoltaic detector, ACS Nano 12 (2018) 425–431, https://doi.org/10.1021/acsnano.7b06633.
[7] S. Zhou, X. Liu, H. Yan, Z. Chen, Y. Liu, S. Liu, Highly efficient GaN-based high-power flip-chip light-emitting diodes, Opt Express 27 (2019) A669–A692, https://doi.org/10.1364/OE.27.00A669.
[8] R. Xu, P. Chen, J. Zhou, Y. Li, Y. Li, T. Zhu, K. Cheng, D. Chen, Z. Xie, J. Ye, B. Liu, X. Xiu, P. Han, Y. Shi, R. Zhang, Y. Zheng, High power figure-of-merit, 10.6-kV AlGaN/GaN lateral Schottky barrier diode with single channel and sub-100-microm anode-to-cathode spacing, Small (2022), 2107301, https://doi.org/10.1002/smll.202107301.
[9] J. He, W.C. Cheng, Q. Wang, K. Cheng, H. Yu, Y. Chai, Recent advances in GaN-based power HEMT devices, Adv. Electron. Mater. 7 (2021), https://doi.org/10.1002/aelm.202001045, 2001045.
[10] K. Kanegae, M. Kaneko, T. Kimoto, M. Horita, J. Suda, Characterization of carrier concentration and mobility of GaN bulk substrates by Raman scattering and infrared reflectance spectroscopies, Jpn. J. Appl. Phys. 57 (2018), 070309, https://doi.org/10.7567/jjap.57.070309.
[11] M. Chafai, A. Jaouhari, A. Torres, R. Antón, E. Martın, J. Jiménez, W.C. Mitchel, Raman scattering from LO phonon-plasmon coupled modes and Hall-effect in n-type silicon carbide 4H–SiC, J. Appl. Phys. 90 (2001) 5211–5215, https://doi.org/10.1063/1.1410884.
[12] A. Mooradian, G.B. Wright, Observation of the interaction of plasmons with longitudinal optical phonons in GaAs, Phys. Rev. Lett. 16 (1966) 999–1001, https://doi.org/10.1103/PhysRevLett.16.999.
[13] A. Mooradian, A.L. McWhorter, Polarization and intensity of Raman scattering from plasmons and phonons in gallium arsenide, Phys. Rev. Lett. 19 (1967) 849–852, https://doi.org/10.1103/PhysRevLett.19.849.
[14] M.V. Klein, B.N. Ganguly, P.J. Colwell, Theoretical and experimental study of Raman scattering from coupled LO-phonon-plasmon modes in silicon carbide, Phys. Rev. B 6 (1972) 2380–2388, https://doi.org/10.1103/PhysRevB.6.2380.
[15] R. Ruppin, J. Nahum, Phonon-plasmon modes in small GaN crystals, J. Phys. Chem. Solid. 35 (1974) 1311–1315, https://doi.org/10.1016/s0022-3697(74)80156-3.
[16] K. Narita, Y. Hijikata, H. Yaguchi, S. Yoshida, S. Nakashima, Characterization of carrier concentration and mobility in n-type SiC wafers using infrared reflectance spectroscopy, Jpn. J. Appl. Phys. 43 (2004) 5151–5156, https://doi.org/10.1143/jjap.43.5151.
[17] F. Demangeot, J. Frandon, M.A. Renucci, C. Meny, O. Briot, R.L. Aulombard, Interplay of electrons and phonons in heavily doped GaN epilayers, J. Appl. Phys. 82 (1997) 1305–1309, https://doi.org/10.1063/1.365903.
[18] H. Harima, H. Sakashita, S. Nakashima, Raman microprobe measurement of under-damped LO-phonon-plasmon coupled mode in n-type GaN, Mater. Sci. Forum (1998) 264–268, https://doi.org/10.4028/www.scientific.net/MSF.264-268.1363, 1363-1366.
[19] Z.F. Li, W. Lu, H.J. Ye, Z.H. Chen, X.Z. Yuan, H.F. Dou, S.C. Shen, G. Li, S.J. Chua, Carrier concentration and mobility in GaN epilayers on sapphire substrate studied by infrared reflection spectroscopy, J. Appl. Phys. 86 (1999) 2691–2695, https://doi.org/10.1063/1.371112.
[20] E. Frayssinet, W. Knap, S. Krukowski, P. Perlin, P. Wisniewski, T. Suski, I. Grzegory, S. Porowski, Evidence of free carrier concentration gradient along the c-axis for undoped GaN single crystals, J. Cryst. Growth 230 (2001) 442–447, https://doi.org/10.1016/S0022-0248(01)01294-5.
[21] L.H. Robins, E. Horneber, N.A. Sanford, K.A. Bertness, M.D. Brubaker, J. B. Schlager, Raman spectroscopy based measurements of carrier concentration in n-type GaN nanowires grown by plasma-assisted molecular beam epitaxy, J. Appl. Phys. 120 (2016), 124313, https://doi.org/10.1063/1.4963291.
[22] B. Ma, M. Tang, K. Ueno, A. Kobayashi, K. Morita, H. Fujioka, Y. Ishitani, Combined infrared reflectance and Raman spectroscopy analysis of Si-doping limit of GaN, Appl. Phys. Lett. 117 (2020), 192103, https://doi.org/10.1063/5.0023112.
[23] W. Zheng, R.S. Zheng, F. Huang, H.L. Wu, F.D. Li, Raman tensor of AlN bulk single crystal, Photon. Res. 3 (2015) 38–43, https://doi.org/10.1364/Prj.3.000038.
[24] D. Wang, C.C. Tin, J.R. Williams, M. Park, Y.S. Park, C.M. Park, T.W. Kang, W. C. Yang, Raman characterization of electronic properties of self-assembled GaN nanorods grown by plasma-assisted molecular-beam epitaxy, Appl. Phys. Lett. 87 (2005), 242105, https://doi.org/10.1063/1.2146066.
[25] B.B. Varga, Coupling of plasmons to polar phonons in degenerate semiconductors, Phys. Rev. 137 (1965) A1896–A1902, https://doi.org/10.1103/PhysRev.137.A1896.
[26] B. Ma, D. Jinno, H. Miyake, K. Hiramatsu, H. Harima, Orientation dependence of polarized Raman spectroscopy for nonpolar, semi-polar, and polar bulk GaN substrates, Appl. Phys. Lett. 100 (2012), 011909, https://doi.org/10.1063/1.3674983.
[27] B. Kosicki, R. Powell, J. Burgiel, Optical absorption and vacuum-ultraviolet reflectance of GaN thin films, Phys. Rev. Lett. 24 (1970) 1421, https://doi.org/10.1103/PhysRevLett.24.1421.
[28] G. Irmer, V. Toporov, B. Bairamov, J. Monecke, Determination of the charge carrier concentration and mobility in n-gap by Raman spectroscopy, Phys. Status Solidi 119 (1983) 595–603, https://doi.org/10.1002/pssb.2221190219.
[29] H. Yugami, S. Nakashima, A. Mitsuishi, A. Uemoto, M. Shigeta, K. Furukawa, A. Suzuki, S. Nakajima, Characterization of the free-carrier concentrations in doped β-SiC crystals by Raman scattering, J. Appl. Phys. 61 (1987) 354–358, https://doi.org/10.1063/1.338830.
[30] M. Suzuki, T. Uenoyama, A. Yanase, First-principles calculations of effective-mass parameters of AlN and GaN, Phys. Rev. B Condens. Matter 52 (1995) 8132–8139, https://doi.org/10.1103/physrevb.52.8132.
[31] P. Perlin, E. Litwin-Staszewska, B. Suchanek, W. Knap, J. Camassel, T. Suski, R. Piotrzkowski, I. Grzegory, S. Porowski, E. Kaminska, J.C. Chervin, Determination of the effective mass of GaN from infrared reflectivity and Hall effect, Appl. Phys. Lett. 68 (1996) 1114–1116, https://doi.org/10.1063/1.115730.
[32] L. Cheng, S. Zhu, W. Zheng, F. Huang, Ultra-wide spectral range (0.4–8 μm) transparent conductive ZnO bulk single crystals: a leading runner for mid-infrared optoelectronics, Mater. Today Phys. 14 (2020), 100244, https://doi.org/10.1016/j.mtphys.2020.100244.
[33] L. Cheng, W. Zheng, L. Jia, F. Huang, Quasiphonon polaritons, Heliyon 6 (2020), e05277, https://doi.org/10.1016/j.heliyon.2020.e05277.
[34] M. Born, E. Wolf, Principles of Optics: Electromagnetic Theory of Propagation, Interference and Diffraction of Light, Elsevier, 2013.
[35] S. Zhu, W. Zheng, X. Lu, L. Cheng, W. Zhong, F. Huang, Identification of TO and LO phonons in cubic natBP, 10BP and 11BP crystals, Appl. Phys. Lett. 118 (2021), 162106, https://doi.org/10.1063/5.0048871.
[36] H. Harima, Properties of GaN and related compounds studied by means of Raman scattering, J Phys-Condens Mat 14 (2002) R967–R993, https://doi.org/10.1088/0953-8984/14/38/201.
[37] P. Perlin, C. Jauberthie-Carillon, J.P. Itie, A. San Miguel, I. Grzegory, A. Polian, Raman scattering and x-ray-absorption spectroscopy in gallium nitride under high pressure, Phys. Rev. B 45 (1992) 83–89, https://doi.org/10.1103/PhysRevB.45.83.
[38] V.Y. Davydov, Y.E. Kitaev, I.N. Goncharuk, A.N. Smirnov, J. Graul, O. Semchinova, D. Uffmann, M.B. Smirnov, A.P. Mirgorodsky, R.A. Evarestov, Phonon dispersion and Raman scattering in hexagonal GaN and AlN, Phys. Rev. B 58 (1998) 12899–12907, https://doi.org/10.1103/PhysRevB.58.12899.
[39] Y. Fan, W. Zheng, S. Zhu, L. Cheng, H. Qi, L. Li, F. Huang, Extraction of carrier concentration and mobility of ZnO by mid-infrared reflectance spectroscopy, J. Lumin. 239 (2021), 118365, https://doi.org/10.1016/j.jlumin.2021.118365.
[40] S. Nakashima, H. Harima, Spectroscopic analysis of electrical properties in polar semiconductors with over-damped plasmons, J. Appl. Phys. 95 (2004) 3541–3546, https://doi.org/10.1063/1.1655681.
[41] H. Iwata, K.M. Itoh, Donor and acceptor concentration dependence of the electron Hall mobility and the Hall scattering factor in n-type 4H– and 6H–SiC, J. Appl. Phys. 89 (2001) 6228–6234, https://doi.org/10.1063/1.1366660.